

The Simulation of Switched Capacitor Circuits

Using Spice AC Simulation (Version 1)

Christian Enz (christian.enz@epfl.ch)

2025-06-20

Table of contents

| | | |
|----------|---|-----------|
| 1 | Introduction | 3 |
| 2 | Simulation of SC circuits with Spice | 4 |
| 2.1 | Continuous-time model of a switched-capacitor | 4 |
| 2.2 | Approximation of time delay in ngspice | 5 |
| 3 | Example 1: First-order passive low-pass filter | 9 |
| 3.1 | Simulations | 10 |
| 3.1.1 | LTSpice | 10 |
| 3.1.2 | ngspice | 12 |
| 4 | Example 2: First-order active low-pass filter | 16 |
| 4.1 | Simulations | 18 |
| 4.1.1 | LTSpice | 18 |
| 4.1.2 | ngspice | 18 |
| 5 | Example 3: Third-order active low-pass filter | 21 |
| 5.1 | Simulations | 23 |
| 5.1.1 | LTSpice | 23 |
| 5.1.2 | ngspice | 25 |
| 6 | Conclusion | 26 |
| | References | 27 |

1 Introduction

This notebook presents how to simulate switched-capacitor (SC) circuits and particularly filters in the frequency domain with AC simulation using Spice simulator such as LTSpice [1] or ngspice [2]. The following theory is based on [3] [4]. Because SC circuits are not linear time invariant (non-LTI), they normally cannot be simulated in AC with a conventional Spice circuit simulator. However, we can use the special library that was developed by C. Enz for the AC simulation of SC circuit with two 50% duty-cycle non-overlapping clocks. This library basically simulates the circuits in phase Φ_1 and Φ_2 concurrently and then insures the charge conservation between the two circuits of phase Φ_1 and phase Φ_2 .

i Note

The library for LTSpice includes symbols that can be used for schematic capture of SC circuits making the simulations of SC circuits straightforward.

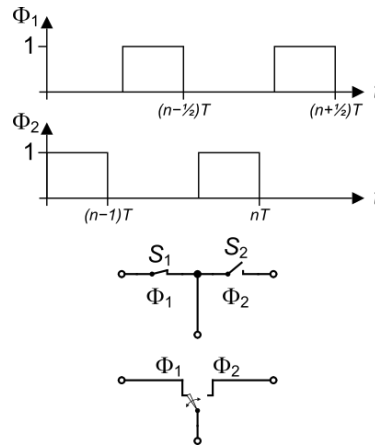


Figure 1.1: Two switches controlled by two non-overlapping phases and the equivalent toggle switch.

We will focus on two phases SC circuits which operate with two non-overlapping phases Φ_1 and Φ_2 as shown in Figure 1.1. Phase Φ_1 controls switch S_1 , whereas phase Φ_2 controls switch S_2 . Switch S_1 is closed when phase Φ_1 is high and switch S_2 is closed when phase Φ_2 is high. Since phase Φ_1 and Φ_2 are non-overlapping, it means that switches S_1 and S_2 are never closed at the same time avoiding any short-circuit between the input and output. This means that they can be replaced by a toggle switch as shown in Figure 1.1.

We start describing the technique used for AC simulation in Spice and illustrate it with the design of various filters.

2 Simulation of SC circuits with Spice

2.1 Continuous-time model of a switched-capacitor

SC circuits are linear circuits but they are not time-invariant (LTI) because the circuit during one phase (say phase Φ_1) is not the same than the circuit in other phases (say Φ_2 for a two phases system). However, the circuit in each phase is LTI and can be simulated with Spice. The basic idea for a two non-overlapping phases SC circuit is to enter the netlist corresponding to each phase Φ_1 and Φ_2 and couple them with a special SC component that ensures the charge conservation between the two phases.

Let's consider a SC as shown in the left figure of Figure 2.1 with the phases Φ_1 and Φ_2 shown on top where $T = 1/f_s$ is the sampling period and D the duty cycle which is usually equal to $1/2$.

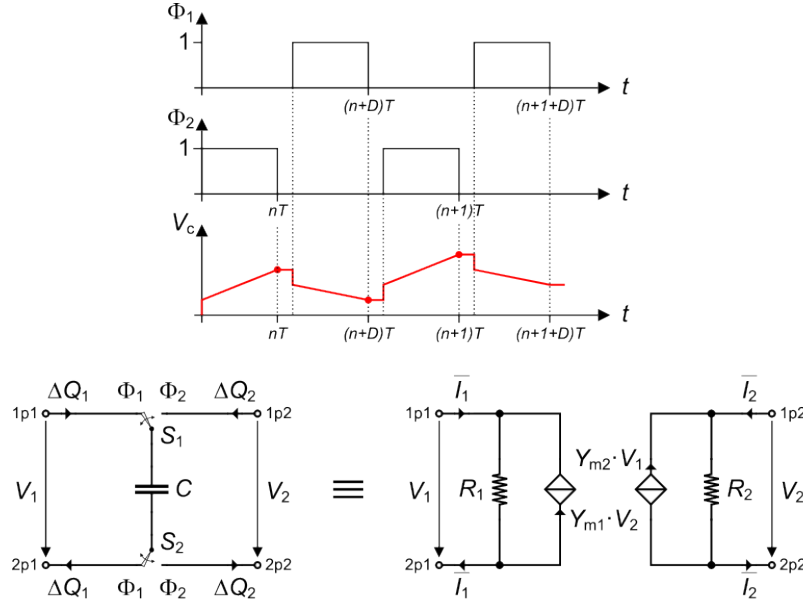


Figure 2.1: Switched-capacitor C and its equivalent continuous-time equivalent.

We can write the following charge conservation equations for capacitor C

$$\Delta Q_1((n+D)T) = C \cdot [V_1((n+D)T^-) - V_2(nT^-)], \quad (2.1)$$

$$\Delta Q_2((n+1)T) = C \cdot [V_2((n+1)T^-) - V_1((n+D)T^-)], \quad (2.2)$$

where ΔQ_1 corresponds to the change of charge on capacitor C between the end of phase Φ_1 and Φ_2 and ΔQ_2 is the change of charge on capacitor C between the end of phase Φ_2 and Φ_1 . The above charge equations can be replaced by the average currents \bar{I}_1 and \bar{I}_2

$$\bar{I}_1 = \frac{C}{T} \cdot [V_1((n+D)T^-) - V_2(nT^-)], \quad (2.3)$$

$$\bar{I}_2 = \frac{C}{T} \cdot [V_2((n+1)T^-) - V_1((n+D)T^-)], \quad (2.4)$$

where the average currents $\overline{I_1}$ and $\overline{I_2}$ are defined by

$$\overline{I_1}((n+D)T) = \frac{1}{T} \cdot \int_{nT}^{(n+D)T} i_c(t) dt = \frac{\Delta Q_1((n+D)T)}{T}, \quad (2.5)$$

$$\overline{I_2}((n+1)T) = \frac{1}{T} \cdot \int_{(n+D)T}^{(n+1)T} i_c(t) dt = \frac{\Delta Q_2((n+1)T)}{T}. \quad (2.6)$$

The currents can then be written in the z -domain as

$$\overline{I_1} = \frac{C}{T} \cdot [V_1(z) - z^{-D} V_2(z)], \quad (2.7)$$

$$\overline{I_2} = \frac{C}{T} \cdot [V_2(z) - z^{-(1-D)} V_1(z)]. \quad (2.8)$$

The above equations can be modelled by the equivalent continuous-time circuit shown on the bottom right of Figure 2.1 where

$$R_1 = R_2 = R_{eq} = \frac{T}{C} \quad (2.9)$$

and

$$Y_{m1} = G_{meq} \cdot e^{-sDT}, \quad (2.10)$$

$$Y_{m2} = G_{meq} \cdot e^{-s(1-D)T}, \quad (2.11)$$

with

$$G_{meq} = \frac{1}{R_{eq}}. \quad (2.12)$$

The continuous-time equivalent is easy to implement in Spice using the Laplace instruction for implementing the time delays e^{-sDT} and $e^{-s(1-D)T}$. This Laplace operator is available in LTSpice but unfortunately it is not available in ngspice. However, we can replace it by using the XSpice `s_xfer` element which allows implementing a transfer function given by a rational function in s provided the order of the denominator is equal or larger than the order of the numerator.

2.2 Approximation of time delay in ngspice

In the implementation of SC circuits with two non-overlapping phases for the simulation with LTSpice, we are using an ideal time delay $e^{s\Delta T}$ where s is the Laplace variable, $\Delta T = D \cdot T$, with $T = 1/f_s$ the sampling period and D is the duty cycle (often equal to $D = 0.5$). This operator is available in LTSpice as `LAPLACE = exp(-s * D * T)` but unfortunately it is not available in ngspice. We can however use the XSpice `s_xfer` model which describes the transfer function given by a rational function in s with the order of the numerator m smaller than the order of the denominator n . There are various ways to approximate a constant delay with a rational function in s . The one that gives the best results is the Pade approximation [5]

$$e^{-s \cdot \Delta T} \cong \frac{\sum_{k=0}^m p_k \cdot (s \cdot \Delta T)^k}{\sum_{k=0}^n q_k \cdot (s \cdot \Delta T)^k} \quad (2.13)$$

The coefficients in the case $m = n$ are given by

$$q_k = \frac{(2n-k)!}{k!(n-k)!}, \quad (2.14)$$

$$p_k = (-1)^k \cdot q_k. \quad (2.15)$$

The corresponding transfer function of the ideal delay is

$$H(\omega) = e^{-j\omega \Delta T} \quad (2.16)$$

with a magnitude and phase given by

$$|H(\omega)| = 1, \quad (2.17)$$

$$\Phi(\omega) = \arg(H(\omega)) = -\omega \Delta T. \quad (2.18)$$

An ideal delay can be characterized by a constant phase delay defined as

$$\tau_{\Phi}(\omega) = -\frac{\Phi(\omega)}{\omega} = \Delta T \quad (2.19)$$

or group delay

$$\tau_{gd}(\omega) = -\frac{d\Phi(\omega)}{d\omega} = \Delta T \quad (2.20)$$

We can evaluate the coefficients for an order $n = 5$.

Table 2.1: Coefficients of $q[k]$ and $p[k]$ for $n = 5$.

| n | p[k] | q[k] |
|---|--------|-------|
| 0 | 30240 | 30240 |
| 1 | -15120 | 15120 |
| 2 | 3360 | 3360 |
| 3 | -420 | 420 |
| 4 | 30 | 30 |
| 5 | -1 | 1 |

The approximations up to order 5 are simulated in LTSpice and compared to the ideal delay also simulated with LTSpice. The results are presented in Figure 2.2.

In the case of $D = 0.5$, the phase delay is equal to 0.5. We see that the approximations progressively extends the phase delay to higher frequency. Since we usually are only interested on frequencies up to the Nyquist frequency $f_2/2$, we observe that a 3rd-order approximation should already be fine.

We can simulate the delay block in ngspice using the s_xfer XSpice description. The simulation results are presented in Figure 2.3.

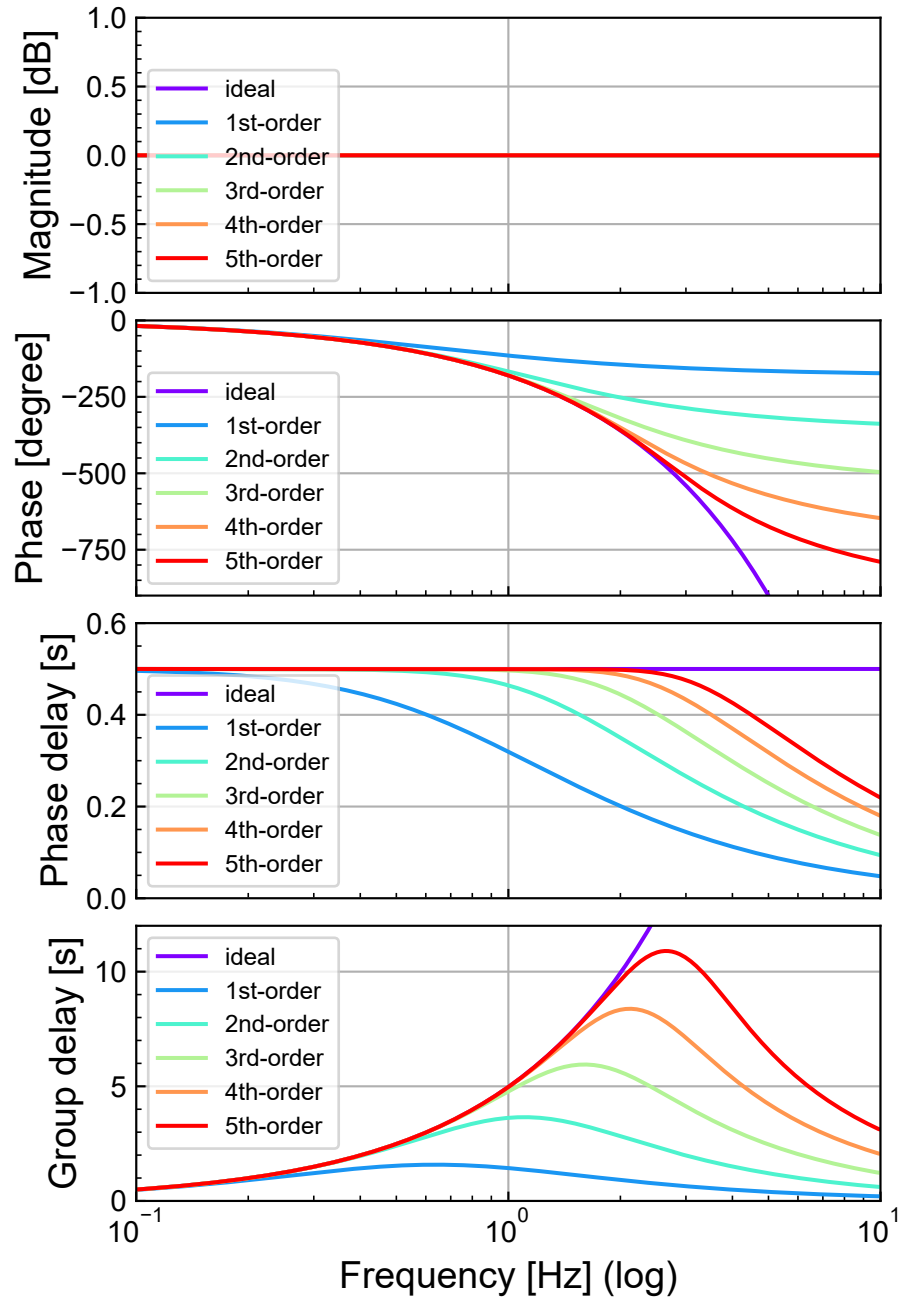


Figure 2.2: Comparison of the delay approximation to the ideal delay.

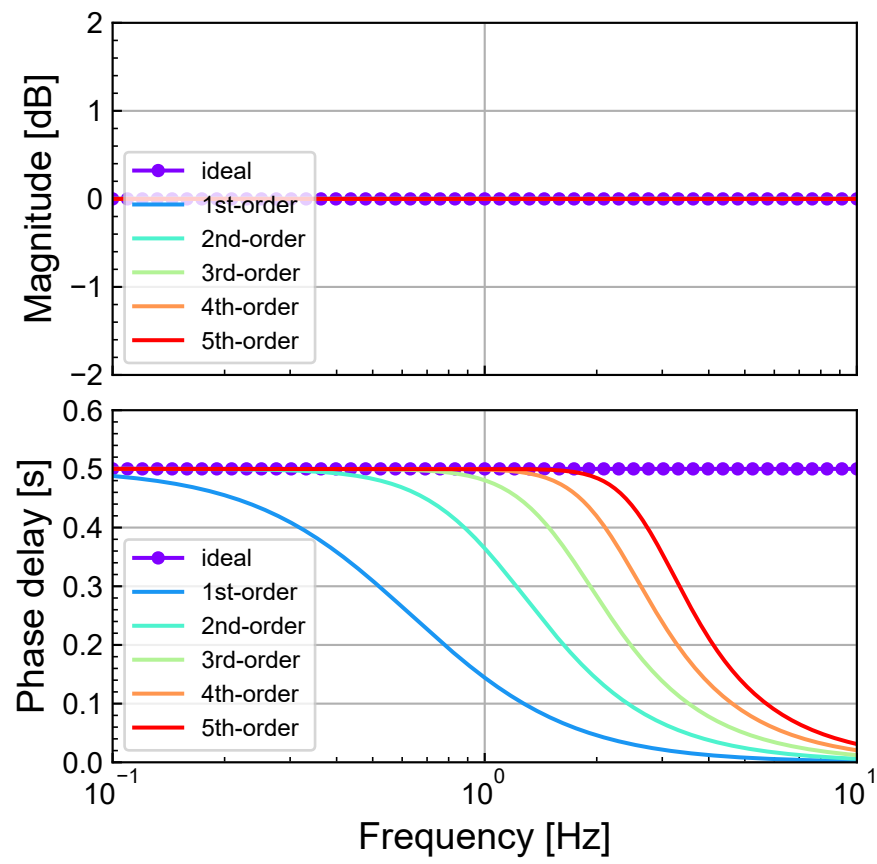


Figure 2.3: Delay approximation with ngspice.

3 Example 1: First-order passive low-pass filter

The simplest example is the implementation of a 1st-order passive RC low-pass filter as illustrated in the left schematic of Figure 3.1.

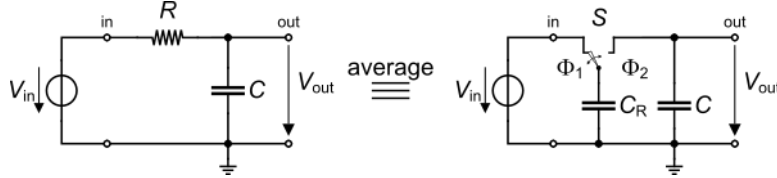


Figure 3.1: Equivalence between 1st-order passive RC and SC filter.

The transfer function of the continuous-time passive RC filter is given by

$$H_a(s) = \frac{1}{1 + s\tau} = \frac{1}{1 + s/\omega_c} \quad (3.1)$$

with $\tau = 1/\omega_c = RC$. The SC equivalent filter is shown on the right of Figure 3.1 where

$$C_R = \alpha \cdot C \quad (3.2)$$

with

$$\alpha = \frac{\omega_c}{f_s} = 2\pi \frac{f_c}{f_s}, \quad (3.3)$$

where f_s is the sampling frequency.

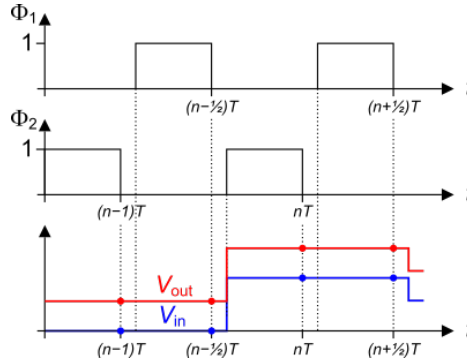


Figure 3.2: Phases and signals for the analysis of the passive SC filter.

Assuming that the output voltage during phase Φ_2 settles to its final value at the end of phase Φ_2 , we can write the charge conservation equation between the end of phase Φ_2 , i.e. time $t = nT$, and the end of phase Φ_1 , i.e. time $(n - 1/2)T$ as

$$(C + C_R) V_{out}(nT) = C_R V_{in}((n - 1/2)T) + C V_{out}((n - 1/2)T). \quad (3.4)$$

Assuming that the input and output voltages change only once per period as shown in Figure 3.2, we have

$$V_{in}((n - 1/2)T) = V_{in}((n - 1)T), \quad (3.5)$$

$$V_{out}((n - 1/2)T) = V_{out}((n - 1)T). \quad (3.6)$$

The above difference equation becomes

$$(C + C_R) V_{out}(nT) = C_R V_{in}((n-1)T) + C V_{out}((n-1)T), \quad (3.7)$$

Taking the z -transform leads to

$$(C + C_R) V_{out}(z) = z^{-1} [C_R V_{in}(z) + C V_{out}(z)] \quad (3.8)$$

which can be solved to derive the z -transfer function of the passive SC filter

$$H(z) = \frac{\alpha z^{-1}}{1 + \alpha - z^{-1}} = \frac{\alpha}{(1 + \alpha)z - 1} \quad (3.9)$$

with

$$\alpha = \frac{C_R}{C}. \quad (3.10)$$

As an example, we want to implement a 1st-order low-pass filter of Figure 3.1 with the parameters given in Table 3.1.

Table 3.1: Parameters for the 1st-order passive low-pass filter of Figure 3.1.

| Specification | Symbol | Value | Unit |
|----------------------|------------------------------------|----------|-------|
| Cut-off frequency | f_c | 1 | kHz |
| Sampling frequency | f_s | 100 | kHz |
| Capacitance | C | 1 | pF |
| Capacitance ratio | $\alpha \triangleq \omega_c / f_s$ | 0.062832 | - |
| Switched-capacitance | C_R | 62.832 | fF |

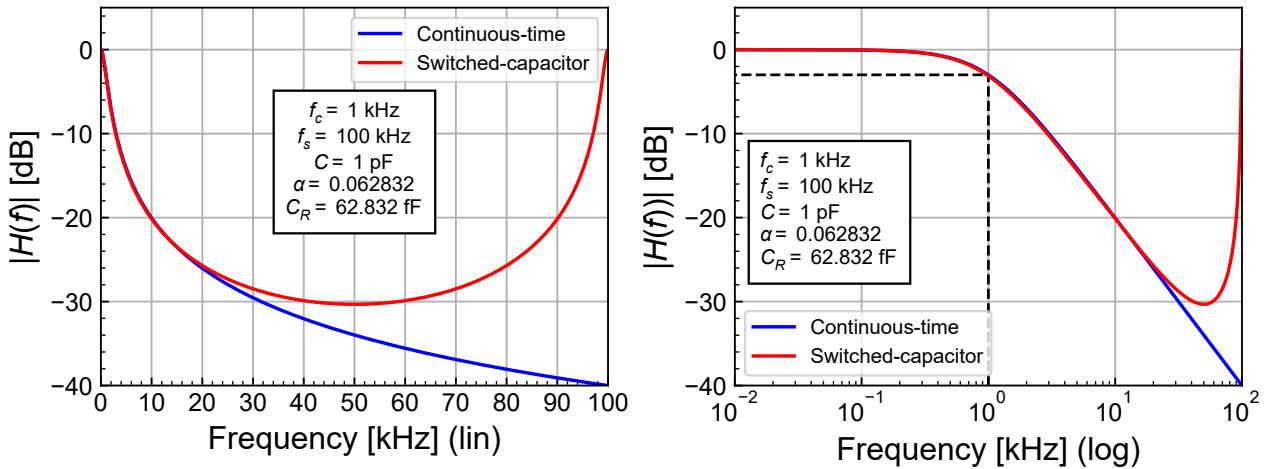


Figure 3.3: Transfer function magnitude of the 1st-order passive low-pass filter of Figure 3.1.

As expected, the magnitude of the transfer function shown in Figure 3.1 is periodic with a period $f_s = 100 \text{ kHz}$. From Figure 3.1, we see that the cut-off frequency of the SC filter is equal to that of the continuous-time (CT) filter. However, because of the sampled-data nature of the SC filter, the transfer function is periodic in f_s . The maximum attenuation is therefore only about 30 dB.

3.1 Simulations

3.1.1 LTSpice

For the LTSpice simulations we can use the schematic shown in Figure 3.4.

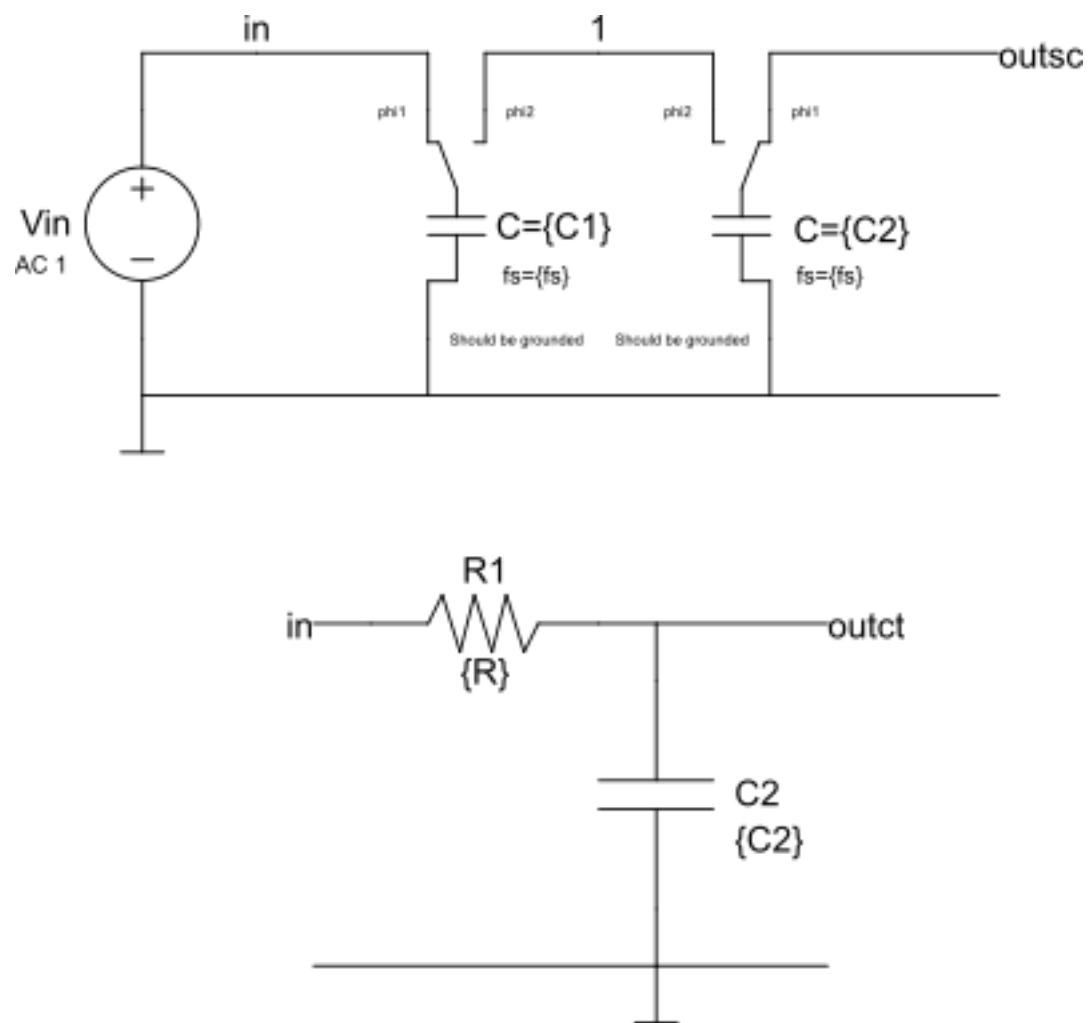


Figure 3.4: LTSpice schematic.

i Note

We may wonder why capacitor C_2 also needs to be modeled by a switched-capacitor in LTSpice despite the fact that it is not really switched. The reason is that we need to define two separate circuits, one that represents the circuit during phase Φ_1 and the other for phase Φ_2 . We cannot have a schematic node, for example node 1 in the above circuit, that is common to the circuit of phase Φ_1 and the circuit of phase Φ_2 . The two separate circuits are then coupled by the implementation of charge conservation between phase Φ_1 and Φ_2 .

We can now simulate the circuit in LTSpice with the same parameters as in Table 3.1.

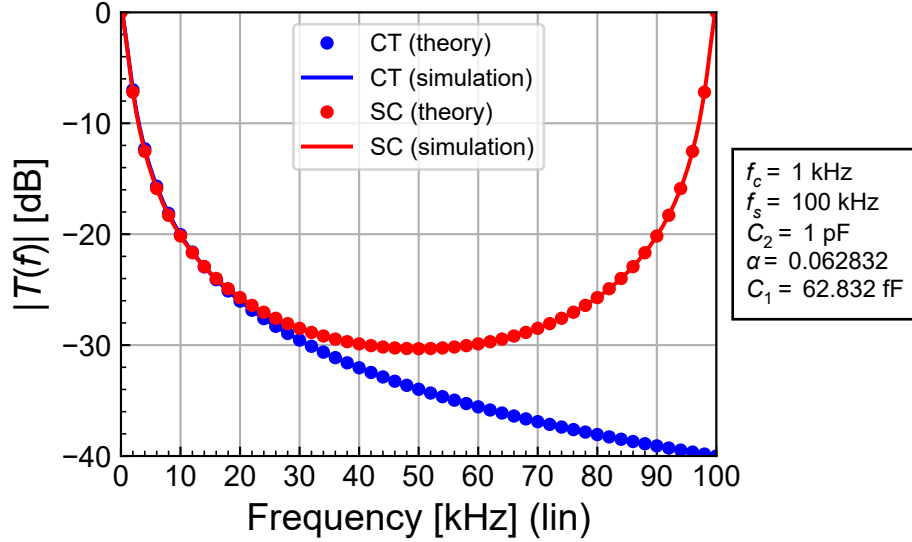


Figure 3.5: Transfer function magnitude of the simulated 1st-order passive low-pass filter of Figure 3.4 with linear x-axis.

With the linear x-axis in Figure 3.5, we can clearly see that the LTSpice AC simulation captures the sampled-data nature of the transfer function of the SC circuit which is now periodic with a period f_s . It then obviously deviates from the CT transfer function for frequencies above about $f_s/10$.

We can now simulate and plot the same circuit but with a log scale to check whether the cut-off frequency is correct.

The results shown in Figure 3.5 and Figure 3.6 show that the simulations perfectly match the theoretical results and that the cut-off frequency is correct and that the asymptotic slope of -20dB/dec above the cut-off frequency is correct as well, up to about $f_s/10$.

We now will now simulate the circuit of Figure 3.4 with the ngspice simulator.

3.1.2 ngspice

We first have a look at the simulations with a linear scale for the frequency axis.

From Figure 3.7, we see that the ngspice simulation perfectly matches the theoretical data.

We can check the effect of the various order for the delay model in ngspice.

We can observe in Figure 3.8 that the 1st-order delay model shows a large discrepancy and is therefore not sufficient. The 2nd-order delay model already does a good job up to the Nyquist frequency which is what we need. The 3rd-order and 4th-order delay models show discrepancy above $3f_s/2$. We will keep the 5th-order delay model since it does not penalize the simulation time.

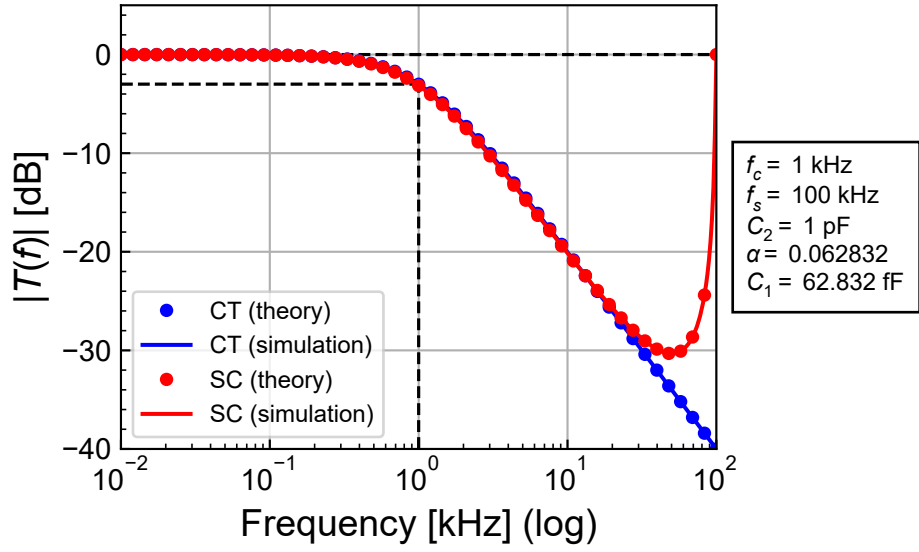


Figure 3.6: Transfer function magnitude of the simulated 1st-order low-pass filter of Figure 3.4 with log x-axis.

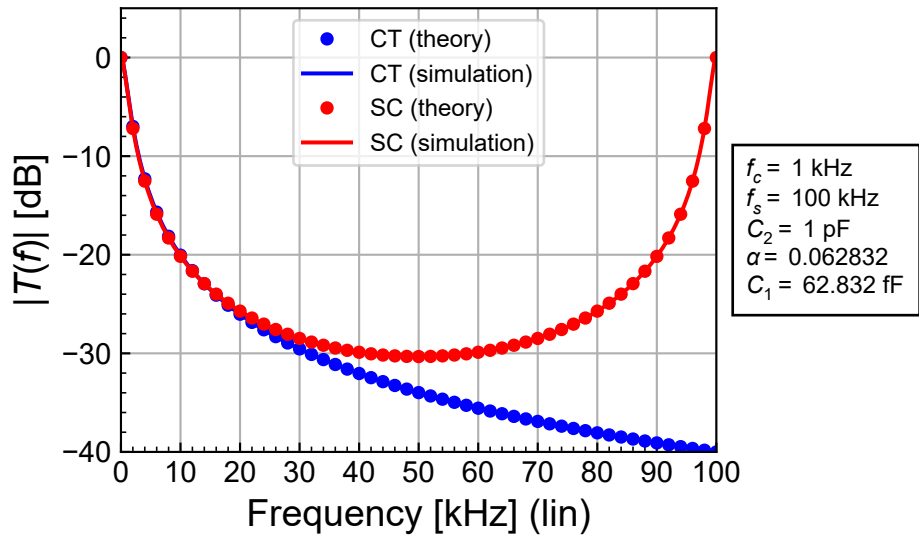


Figure 3.7: Transfer function magnitude of the simulated 1st-order low-pass filter compared to the passive RC circuit with linear x-axis.

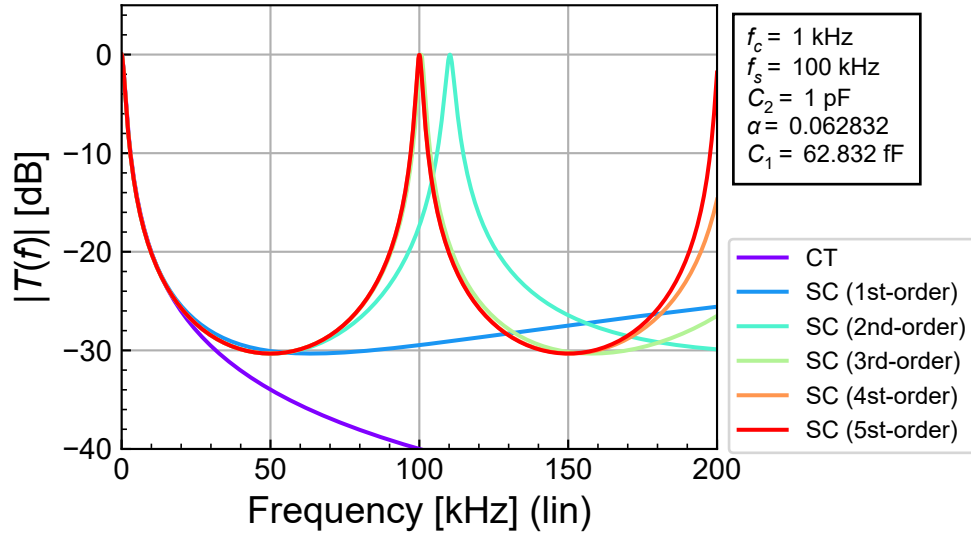


Figure 3.8: ngspice transfer function magnitude simulation of the 1st-order passive low-pass filter with different delay approximation orders.

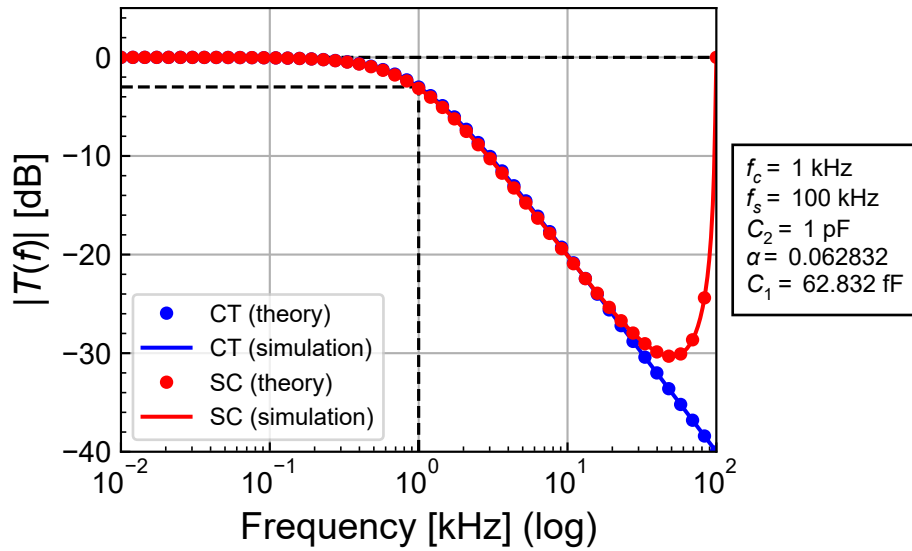


Figure 3.9: Transfer function magnitude of the simulated 1st-order low-pass filter compared to the passive RC circuit with log x-axis.

The plot of Figure 3.9 shows that the ngspice simulation perfectly matches the theoretical result and that the cut-off frequency is correct and that the asymptotic slope of -20dB/dec above the cut-off frequency is correct as well, up to about $f_s/10$.

We can now proceed with the simplest active SC filter, namely a 1st-order LP filter.

4 Example 2: First-order active low-pass filter

The schematic of the general 1st-order SC section is shown in Figure 4.1.

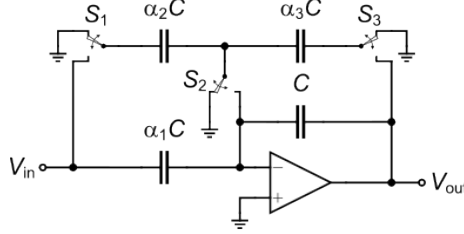


Figure 4.1: 1st-order LP filter with the zero inside the unit circle.

The z -transfer function is given by

$$H(z) = -\frac{(\alpha_1 + \alpha_2)z - \alpha_1}{(1 + \alpha_3)z - 1} \quad (4.1)$$

From the above z -transfer function, we observe that the zero $z_z = \alpha_1/(\alpha_1 + \alpha_2) < 1$ is always inside the unit circle. The corresponding approximate s -domain transfer assuming $z \cong 1 + sT$ is given by

$$H_a(s) \cong -K \cdot \frac{1 + s/\omega_z}{1 + s/\omega_p} \quad (4.2)$$

The approximate design equations for $\omega_z T \ll 1$ and $\omega_p T \ll 1$ are given by

$$\alpha_1 \cong K, \quad (4.3)$$

$$\alpha_2 \cong K \omega_z T, \quad (4.4)$$

$$\alpha_3 \cong \omega_p T. \quad (4.5)$$

With the circuit of Figure 4.1, we cannot disable the zero to implement a simple LP transfer function. Another 1st-order section having the zero outside the unit circle is shown in Figure 4.2.

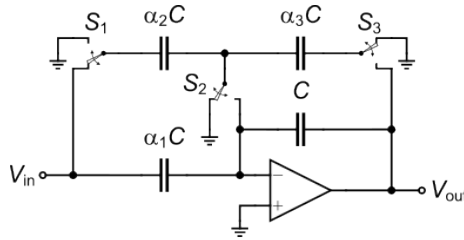


Figure 4.2: 1st-order LP filter with the zero outside the unit circle.

The z -transfer function is given by

$$H(z) = -\frac{\alpha_1 z - (\alpha_1 + \alpha_2)}{(1 + \alpha_3)z - 1} \quad (4.6)$$

From the above z -transfer function, we observe that the zero $z_z = 1 + \alpha_2/\alpha_1 > 1$ is now outside the unit circle. The corresponding approximate s -domain transfer assuming $z \cong 1 + sT$ is given by

$$H_a(s) \cong K \cdot \frac{1 + s/\omega_z}{1 + s/\omega_p} \quad (4.7)$$

The approximate design equations for $\omega_z T \ll 1$ and $\omega_p T \ll 1$ are given by

$$\alpha_1 \cong K \frac{\omega_p T}{\omega_z T}, \quad (4.8)$$

$$\alpha_2 \cong K \omega_p T, \quad (4.9)$$

$$\alpha_3 \cong \omega_p T. \quad (4.10)$$

A LP transfer function without zero can now be implemented setting $\omega_z T \rightarrow \infty$ by choosing $\alpha_1 = 0$. If additionally the gain in the passband is unity $K = 1$, then $\alpha_2 = \alpha_3 = \alpha$ resulting in the schematic shown in Figure 4.3.

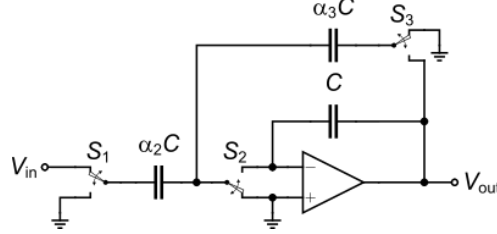


Figure 4.3: 1st-order LP filter.

As an example, we want to implement a 1st-order LP filter with the parameters given in Table 4.1.

Table 4.1: Parameters for the 1st-order low-pass filter of Figure 4.3.

| Specification | Symbol | Value | Unit |
|-------------------------|---|----------|-------|
| Scaling factor | K | 1 | - |
| Cut-off frequency | f_c | 1 | kHz |
| Clock frequency | f_{ck} | 200 | kHz |
| Integrating capacitance | C | 1 | pF |
| Capacitance ratio | $\alpha_2 = \alpha_3 = \alpha = \omega_c T$ | 0.031416 | - |
| Switched-capacitance | $C_2 = \alpha \cdot C$ | 31.416 | fF |
| Switched-capacitance | $C_3 = \alpha \cdot C$ | 31.416 | fF |

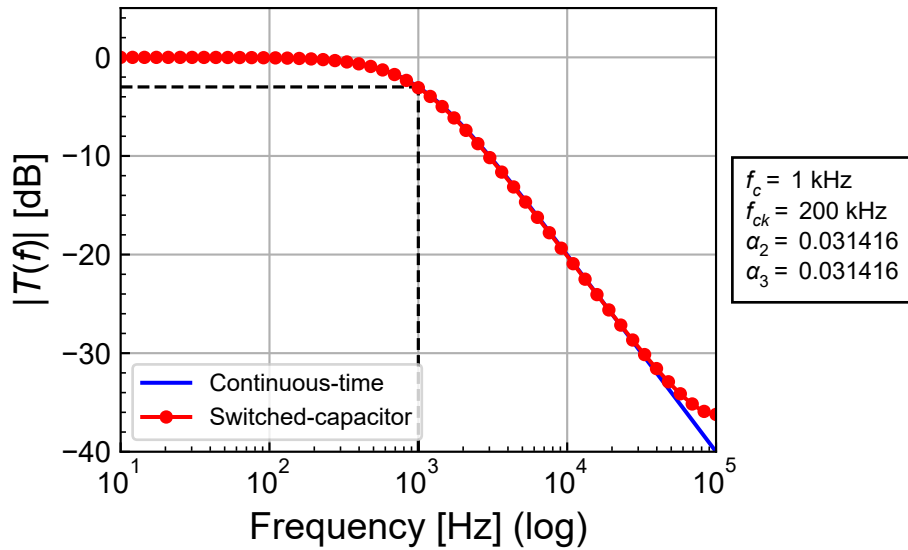


Figure 4.4: Theoretical transfer function of the 1st-order active low-pass filter of Figure 4.3.

4.1 Simulations

For the Spice simulation we will assume that the OPAMP have a DC gain $A = 100$ and infinite bandwidth.

4.1.1 LTSpice

The 1st-order LP SC filter of Figure 4.3 can be simulated in LTSpice using the dedicated library. The corresponding schematic is shown below.

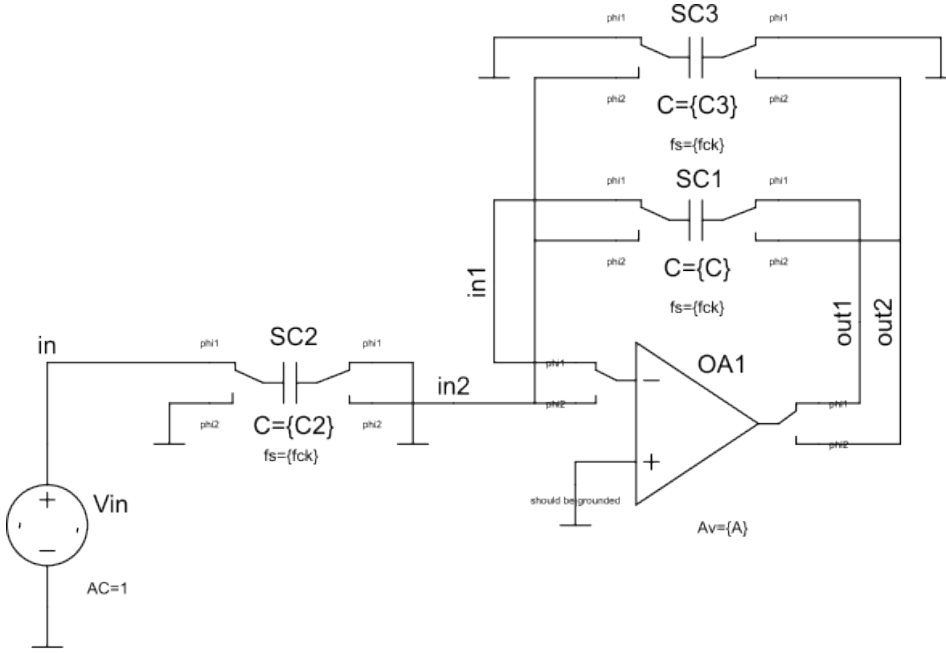


Figure 4.5: Schematic of the 1st-order LP SC filter for LTSpice simulation.

Notice that the integrating capacitor C , which is actually not switched, is also modelled by a switched-capacitor ($SC1$ in the above schematic). As explained above, this is because the circuits during phase Φ_1 and Φ_2 need to be completely separated without any common nodes except the ground. We also need a special amplifier that has two different negative inputs and two different outputs, one for phase Φ_1 and the other for phase Φ_2 .

The simulation result is presented in Figure 4.6 and compared to the theoretical transfer and the continuous-time (CT) equivalent. We see that the simulated transfer function perfectly matches the theoretical transfer function.

We now will simulate the same circuit with ngspice.

4.1.2 ngspice

We simulate the same circuit of Figure 4.5 with ngspice. The simulation result is presented in Figure 4.7 and compared to the theoretical and CT equivalent transfer functions. We can observe that the simulated transfer function perfectly matches the theoretical transfer function.

As shown in Figure 4.8, the ngspice simulation results perfectly match the LTSpice results.

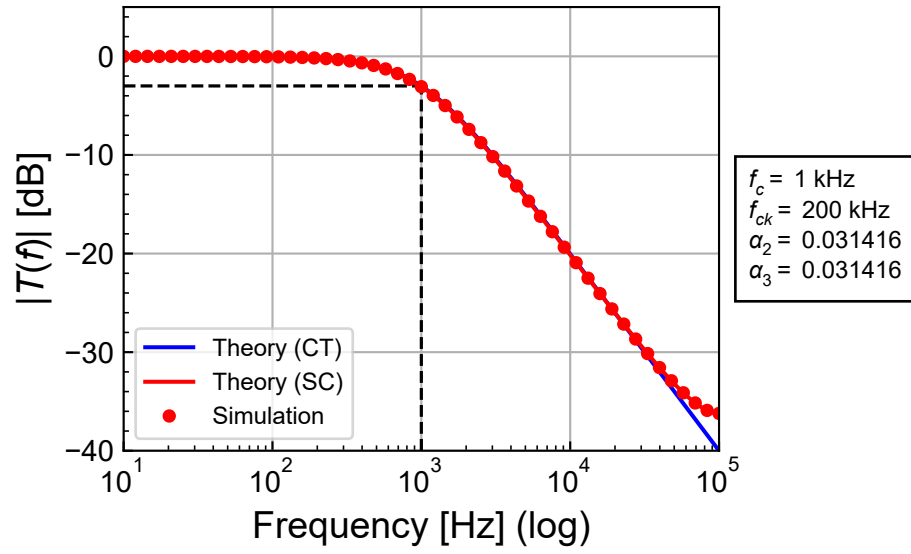


Figure 4.6: Simulated transfer function of the active 1st-order low-pass SC filter of Figure 4.5.

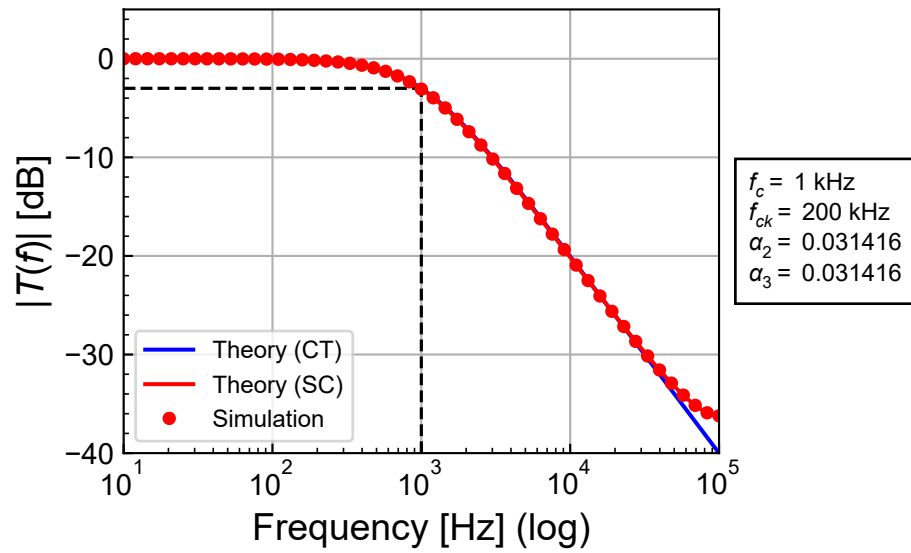


Figure 4.7: Simulated transfer function of the active 1st-order low-pass SC filter of Figure 4.5.

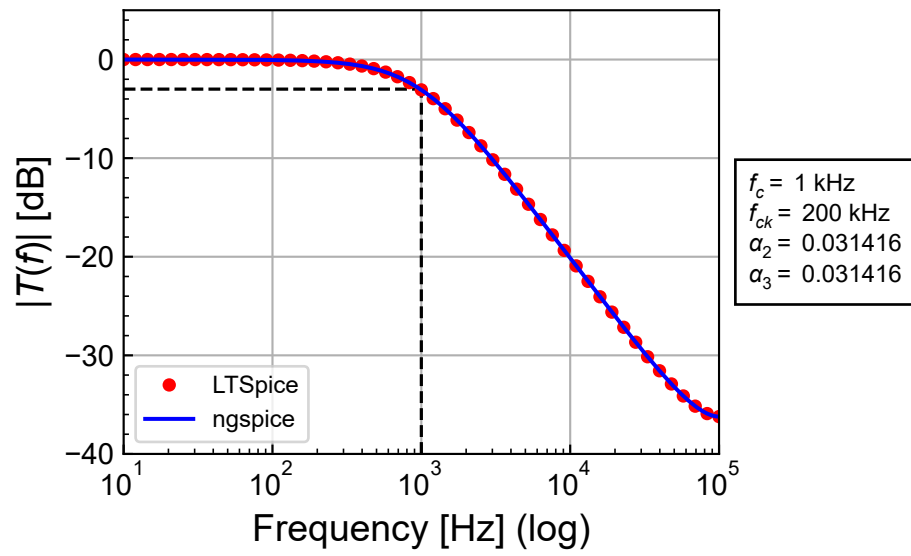


Figure 4.8: Simulated transfer function of the active 1st-order low-pass SC filter of Figure 4.5.

5 Example 3: Third-order active low-pass filter

The last example is the 3rd-order low-pass filter shown in Figure 5.1.

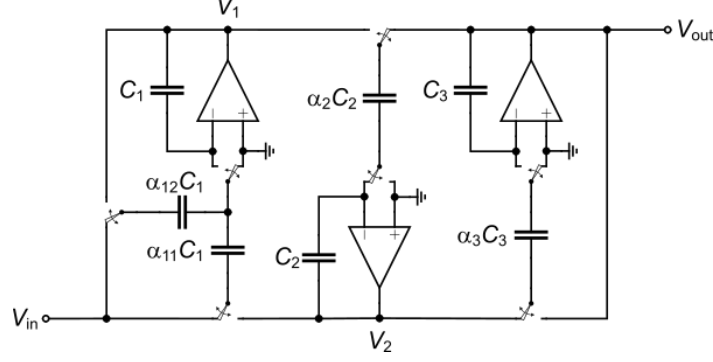


Figure 5.1: Complete 3rd-order SC LP filter including the -6 dB DC gain correction.

From charge conservation analysis, it can be shown that the theoretical transfer function is given by

$$H(z) = \frac{a_2 z^2}{b_3 z^3 + b_2 z^2 + b_1 z + b_0} \quad (5.1)$$

with

$$a_2 = (\alpha_{11} + \alpha_{12}) \alpha_2 \alpha_3, \quad (5.2)$$

$$b_0 = -1, \quad (5.3)$$

$$b_1 = 3 + \alpha_{12} - \alpha_{11} \alpha_2 + \alpha_3 - \alpha_2 \alpha_3, \quad (5.4)$$

$$b_2 = -3 - 2\alpha_{12} + \alpha_{11} \alpha_2 - 2\alpha_3 - \alpha_{12} \alpha_3 + \alpha_2 \alpha_3 + \alpha_{11} \alpha_2 \alpha_3 + \alpha_{12} \alpha_2 \alpha_3, \quad (5.5)$$

$$b_3 = (1 + \alpha_{12})(1 + \alpha_3). \quad (5.6)$$

The specifications of the filter are given in Table 5.1 .

Table 5.1: Specifications of the 3rd-order active low-pass filter.

| Specification | Symbol | Value | Unit |
|---------------------|----------|-------|-------|
| Cut-off frequency | f_p | 20 | kHz |
| Stop-band frequency | f_s | 120 | kHz |
| Clock frequency | f_{ck} | 2 | MHz |
| Pass-band gain | G_p | -1 | dB |
| Stop-band gain | G_s | -40 | dB |

The capacitance ratios for a Chebyshev approximation are given in Table 5.2.

Table 5.2: Capacitance ratios of the 3rd-order active low-pass SC filter of Figure 5.1.

| Symbol | Value | Unit |
|---------------|----------|---------|
| τ_1 | 16.1032 | μs |
| τ_2 | 7.91082 | μs |
| τ_3 | 16.1032 | μs |
| α_{11} | 0.03105 | - |
| α_{12} | 0.03105 | - |
| α_2 | 0.063205 | - |
| α_3 | 0.03105 | - |

The transfer function magnitude corresponding to the parameters given in Table 5.2 is shown in Figure 5.2.

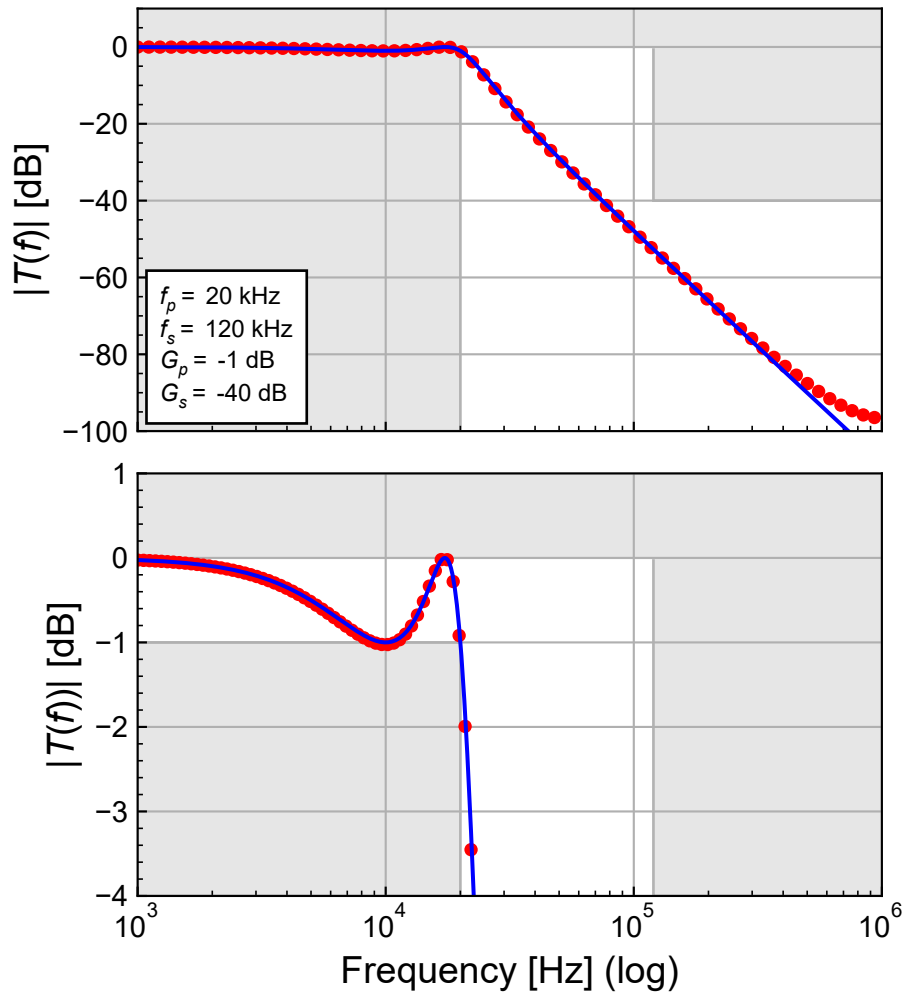


Figure 5.2: Theoretical transfer function magnitude of the 3rd-order active low-pass SC filter of Figure 5.1.

5.1 Simulations

5.1.1 LTSpice

The LTSpice simulations are done with the schematic shown in Figure 5.3 with the capacitance values and capacitance ratios given in Table 5.3.

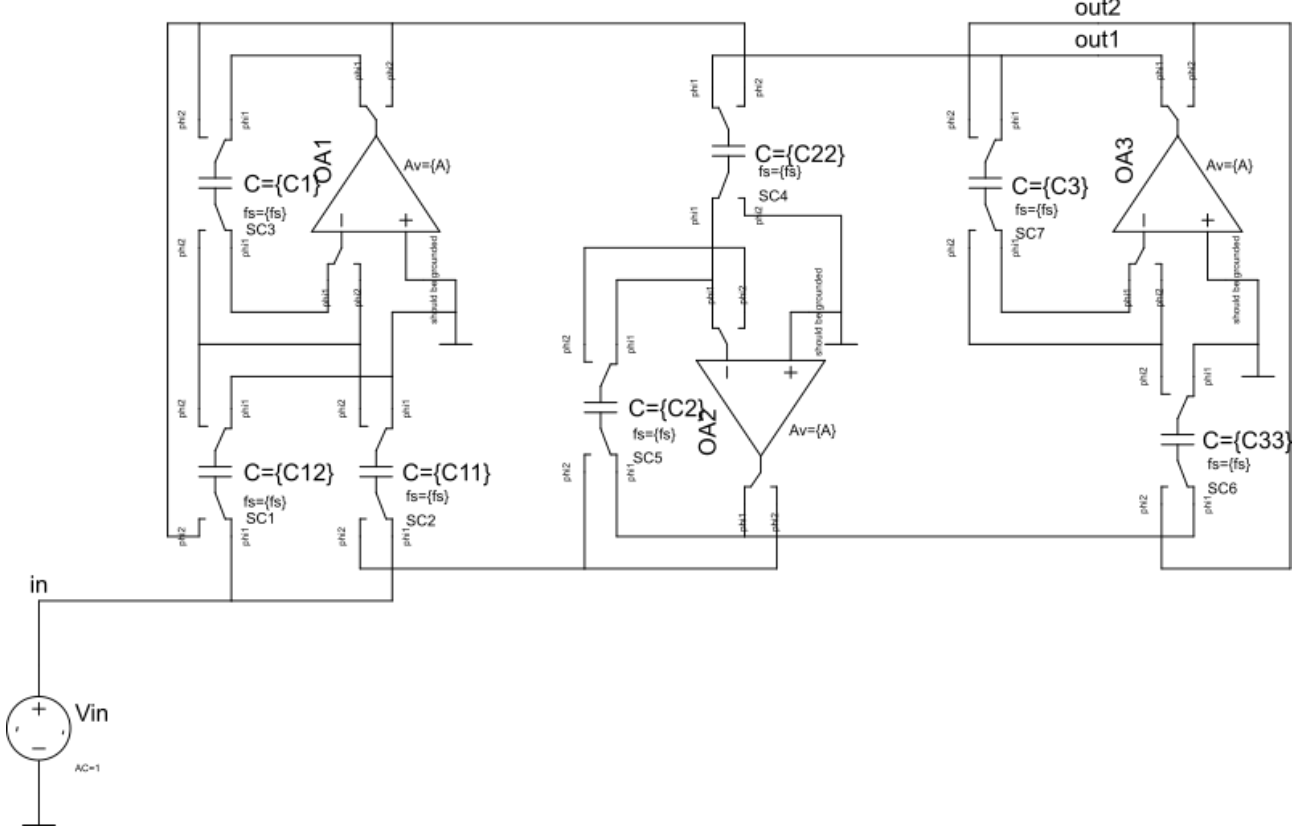


Figure 5.3: Schematic used for the LTSpice simulation.

The simulated magnitude of the transfer function is compared to the theoretical one in Figure 5.4.

Table 5.3: Component values of the 3rd-order active low-pass SC filter of Figure 5.3.

| Symbol | Value | Unit |
|-------------------|----------|-------|
| A | 100 | dB |
| f_{ck} | 2 | MHz |
| C_1 | 3.3 | pF |
| C_2 | 3.3 | pF |
| C_3 | 3.3 | pF |
| α_{11} | 0.03105 | - |
| α_{12} | 0.03105 | - |
| α_2 | 0.063205 | - |
| α_3 | 0.03105 | - |
| $\alpha_{11} C_1$ | 102 | fF |
| $\alpha_{12} C_1$ | 102 | fF |
| $\alpha_2 C_2$ | 209 | fF |
| $\alpha_3 C_3$ | 102 | fF |

From Figure 5.4, we see that the LTSpice simulation perfectly matches the theoretical transfer function.

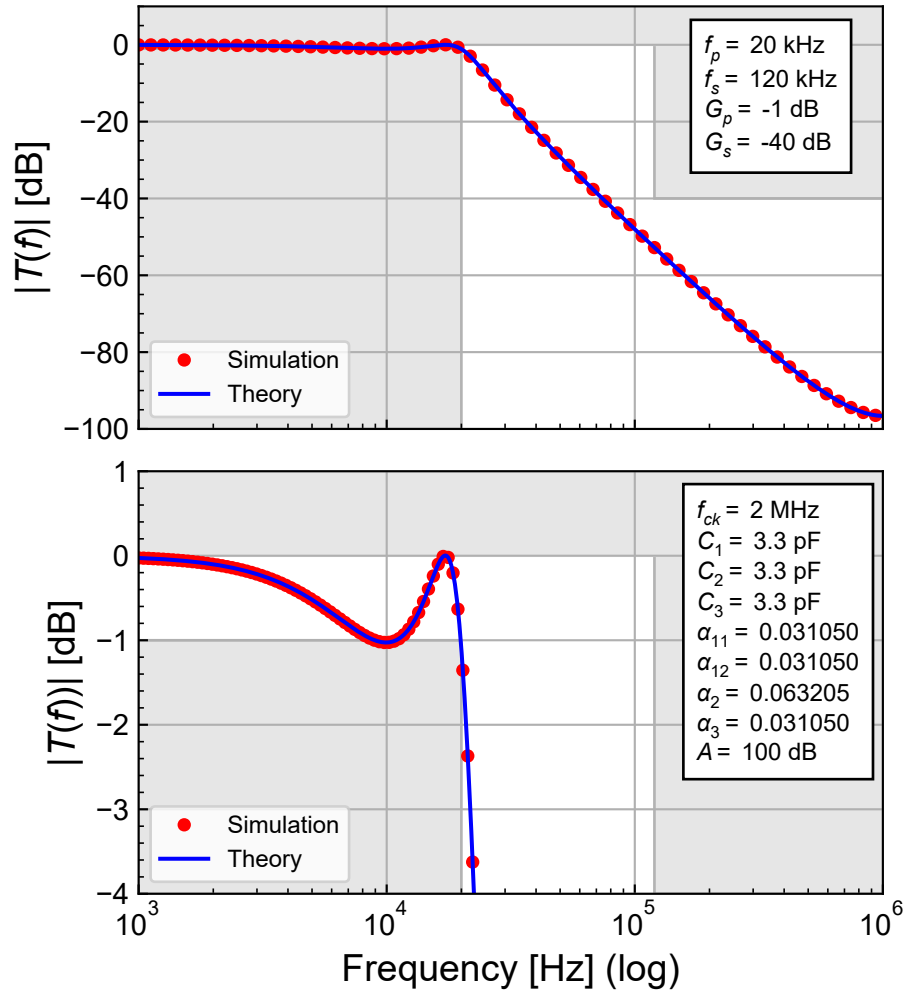


Figure 5.4: Simulated transfer function of the active 3rd-order low-pass SC filter of Figure 5.3.

5.1.2 ngspice

The ngspice simulation is performed with the same circuit as the LTSpice circuit of Figure 5.3 with the same component values of Table 5.3. The ngspice simulation result is presented in Figure 5.5. Similarly to the LTSpice, we see a perfect match between the simulated and the theoretical transfer functions.

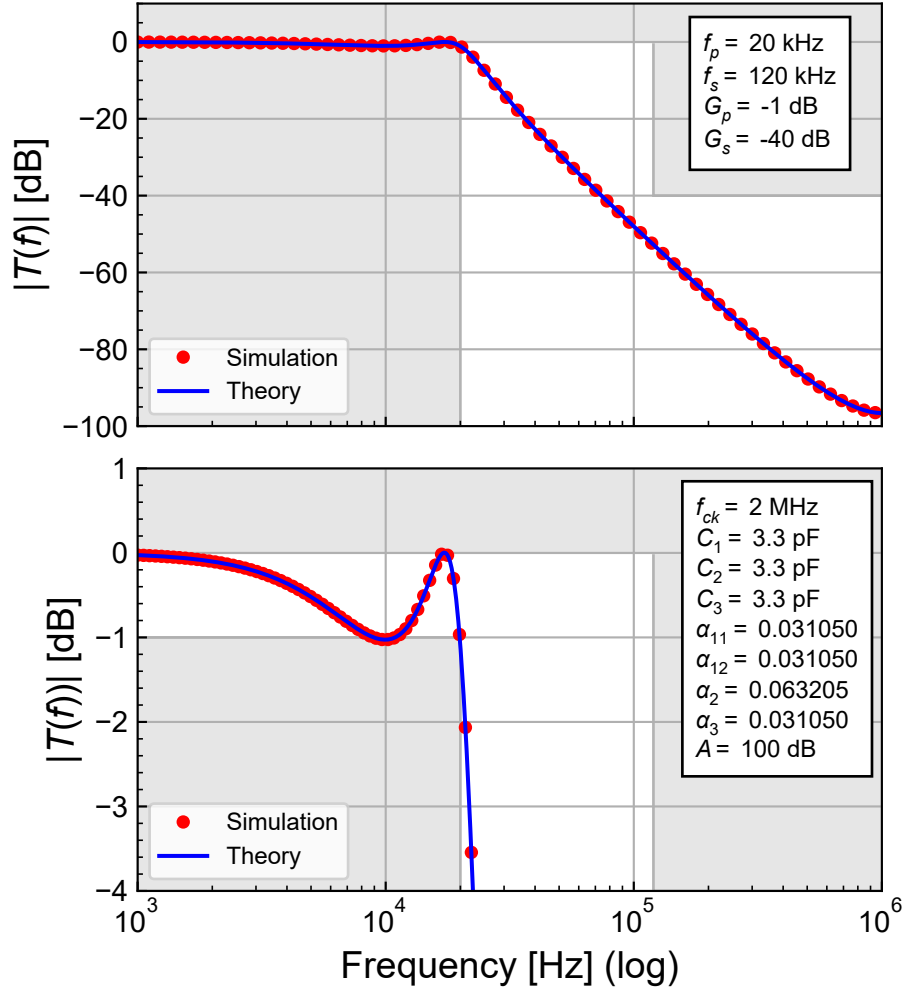


Figure 5.5: Simulated transfer function of the active 3rd-order low-pass SC filter of Figure 5.3.

6 Conclusion

This notebook has presented a technique to simulate SC circuits such as filters using two non-overlapping phases using the AC simulation of a conventional Spice simulator such as LTSpice or ngspice. The circuits during phases Φ_1 and Φ_2 are described separately and run concurrently. They are then coupled by additional component in order to satisfy the charge conservation between phases. A special library has been developed for LTSpice (including the symbols) and ngspice to this purpose. Since the ideal delay operator available in LTSpice does not exist in ngspice, an approximation of the ideal delay has been developed for ngspice using the XSpice `s_xfer` function.

This technique has then been illustrated with several examples starting with the simple passive 1st-order low-pass filter. Then a 1st-order active low-pass filter has been designed and simulated in LTSpice and ngspice. Finally a 3rd-order active SC low-pass filter implementing a Chebyshev approximation has been designed and simulated with LTSpice and ngspice. All the simulated results agree perfectly with the theoretical transfer function demonstrating the validity of the approach.

Of course SC circuits can be simulated in more advanced simulators like Cadence Spectre, but this simple technique allows to quickly verify the design without the need to run a complex simulator.

References

- [1] Analog Devices, “LTSpice.” <https://www.analog.com/en/resources/design-tools-and-calculators/ltspace-simulator.html>, 2025.
- [2] Holger Vogt, Giles Atkinson, Paolo Nenzi, “Ngspice User’s Manual Version 43.” <https://ngspice.sourceforge.io/docs/ngspice-43-manual.pdf>, 2024.
- [3] D. Bielek, V. Biolkova, and Z. Kolka, “AC Analysis of Idealized Switched-Capacitor Circuits in Spice-Compatible Programs,” in *Proceedings of the 11th WSEAS international conference on circuits*, <https://www.wseas.us/e-library/conferences/2007csc/papers/561-533.pdf>, 2007, pp. 223–227.
- [4] D. Bielek, V. Biolkova, and Z. Kolka, “AC Analysis of Real Circuits with External Switching in PSpice,” in *Proceedings of the 12th WSEAS international conference on circuits*, <https://www.wseas.us/e-library/conferences/2007csc/papers/561-533.pdf>, 2008, pp. 193–196.
- [5] L. Pekar and E. Kureckova, “Rational Approximations for Time-Delay Systems: Case Studies,” in *Proceedings of the 13th WSEAS international conference on mathematical and computational methods in science and engineering*, https://www.researchgate.net/publication/262392699_Rational_approximations_for_time-delay_systems_case_studies, 2011, pp. 217–222.